An exploratory Olink proteomic analysis identifies thrombopoietin (THPO) as the predominant protein altered during selinexor maintenance.

Abstract

This exploratory proteomic substudy uses paired plasma samples from the terminated ALLG MM23 trial to investigate Selinexor-attributable systemic proteomic changes in the peripheral plasma of patients with multiple myeloma after autologous stem cell transplantation (ASCT). The parent trial from which these samples were obtained, ALLG MM23, investigated the effects of once-weekly selinexor added to post-ASCT lenalidomide maintenance in patients with multiple myeloma (Rees et al.). ALLG MM23 was terminated early for futility (HR 1.14, p = 0.69) and increased toxicity in the selinexor arm (Rees et al.). In the full randomised population (n = 149), grade ≥3 thrombocytopenia occurred in 26% of the selinexor arm versus 2% in the control arm (Rees et al.). An Olink Reveal panel, consisting of 1,034 assays, was used to analyse paired longitudinal plasma samples collected from a sub-cohort of 38 patients: 19 on the Selinexor plus lenalidomide arm and 19 on the lenalidomide monotherapy arm. Samples were collected at two time points: post-transplant baseline and six months. No candidate assays were nominated for investigation a priori.

1,033 of 1,034 assays passed quality control and were carried forward to analysis. Interaction was modelled in limma using an arm × time interaction with plate control normalisation and patient blocking. Significance was set at a 5% false-discovery rate under Benjamini–Hochberg correction. Only thrombopoietin (THPO) cleared correction, +1.197 $\log_2$ (95% CI 0.778–1.615; q = 2.33×10^{-4}). All 19 patients in the Selinexor arm had a non-negative change in THPO (median +1.013, IQR +0.671 to +1.548, range +0.010 to +2.596), compared with 9 of 19 controls.

This correlative sub-study explores whether six months of maintenance Selinexor leaves a measurable systemic footprint. If so, where does this footprint fall within physiology, and what are its implications? THPO is carried forward as the focus of discussion. All mechanistic interpretation is post hoc and hypothesis-generating. The dataset also reveals numerous potential avenues for further investigation, particularly within the immune-inflammatory axis.

1. Introduction

1.1 Two sides of the same coin — why cancer drugs hurt the host

Clinical oncology operates within a narrow therapeutic index. Anti-neoplastic agents must achieve sufficient cytotoxicity against malignant cells while minimising harm to healthy host tissue. The term "cancer drug" is effectively a mechanistic misnomer, given that most anti-neoplastic agents lack true selectivity and instead act on targets shared by malignant and healthy cells. Selinexor targets exportin-1 (XPO1), a karyopherin essential for the export of over 200 protein and RNA cargoes from the nucleus to the cytoplasm (Argueta et al.). XPO1 is expressed in human tissues, both healthy and malignant (Walker et al.). The difference is that malignant cells, such as myeloma clones, have been found to overexpress XPO1 (Argueta et al.). This shared expression points towards the broad toxicity profile of selinexor. Mechanistically, selinexor works by forming a slowly reversible covalent bond with cysteine 528 in the XPO1 cargo-binding pocket, preventing nuclear export of XPO1-dependent cargoes (Kaser et al.; Machlus et al.). This inhibition of XPO1 leads to the accumulation of tumour suppressors in the nucleus, thereby driving cell-cycle arrest and apoptosis in malignant cells (Tai et al.).

1.2 Multiple myeloma, ALLG MM23, and the gap its closure left

Multiple myeloma is a haematological malignancy characterised by clonal proliferation of plasma cells (Argueta et al.; Tai et al.). Myeloma remains largely incurable, with most patients eventually developing resistance to multiple drugs and inevitably experiencing relapse (Tai et al.). As such, maintenance therapy after ASCT represents a critical therapeutic window to suppress residual disease and prolong progression-free survival.

This exploratory study analyses longitudinal plasma samples from the ALLG MM23 phase 3 trial, which investigated whether adding once-weekly Selinexor to standard post-transplant lenalidomide maintenance prolonged remission in patients with newly diagnosed myeloma (Figure 1) (Rees et al.). The trial was terminated after a planned futility analysis demonstrated no progression-free survival benefit (HR 1.14, 95% CI 0.59–2.22, $p = 0.69$) and significantly higher toxicity in the Selinexor arm (grade ≥3 adverse events in 85% of patients versus 45% on lenalidomide alone, $p < 0.001$; Table 1) (Rees et al.). The results of ALLG MM23 have closed the question of Selinexor's efficacy in this setting. The question that remains on the table, however, is the systemic effect of Selinexor therapy. The latter question is the focus of this report.

Circulating plasma proteins offer one window onto that question. A broad plasma proteomic screen samples the shared systemic pool into which many tissues secrete, and can therefore register host-level responses such as cytokine shifts and feedback from a target organ. This sub-study applies this approach to characterise the systemic profile of six months of maintenance Selinexor therapy.

2. Methods

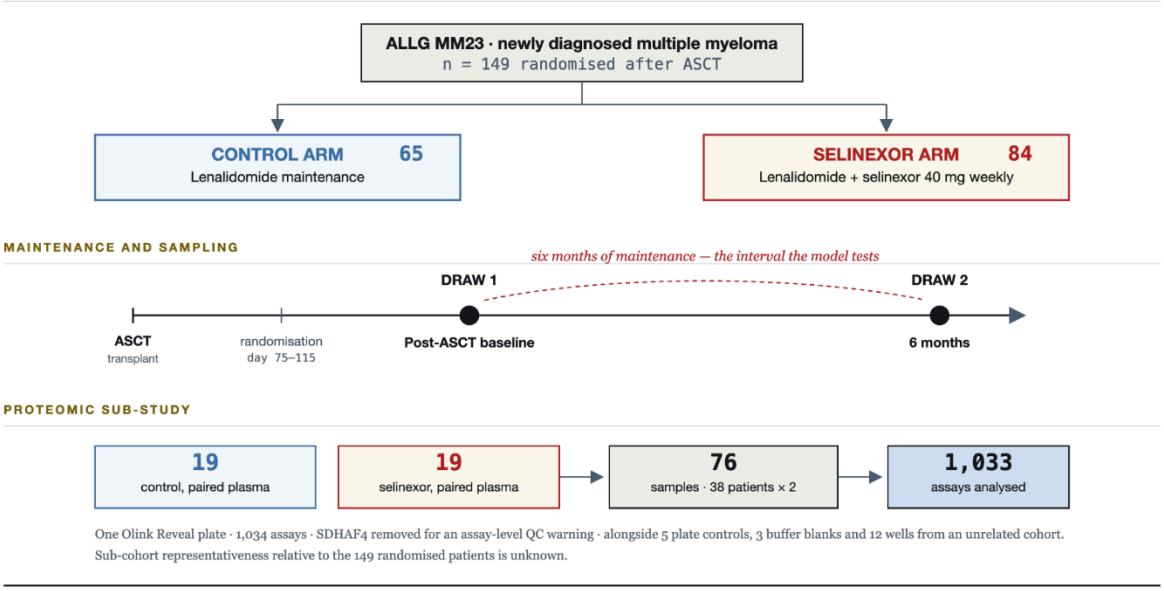

Figure 1. Trial design and sampling schedule. ALLG MM23 (SeaLAND) randomised 149 patients with newly diagnosed multiple myeloma after autologous stem cell transplantation to lenalidomide maintenance alone (n = 65) or lenalidomide plus once-weekly Selinexor with dexamethasone (n = 84). Plasma was drawn at a post-transplant baseline and again after six months of maintenance; the 38 patients with paired draws, 19 per arm, form the sub-cohort analysed here.

Cohort. Paired plasma from 38 MM23 patients, 19 per arm, was collected at two time points: after ASCT and after six months of maintenance therapy (Figure 1). Table 2 describes the full randomised population of 149 patients from which this sub-cohort is drawn (Rees et al.). The representativeness of the sub-cohort is unknown as equivalent characteristics for the 38 contributing patients were unavailable.

Grade ≥3 event	R alone (n = 65)	SR (n = 84)
Thrombocytopenia	2%	26%
Neutropenia	33%	62%
Infection	6%	19%
Gastrointestinal disorders	3%	14%
Fatigue	0%	8%
Any grade ≥3 event	45%	85% (p < 0.001)

Table 1. Grade ≥3 adverse events in ALLG MM23, by arm. Full randomised population (n = 149), not the 38-patient proteomic sub-cohort. R, lenalidomide alone (n = 65); SR, selinexor plus lenalidomide (n = 84). In the 19 SR patients contributing paired plasma, one (5.3%) had recorded grade ≥3 thrombocytopenia. Source: Rees et al.

	R alone (n = 65)	SR (n = 84)
Median age, years (range)	62 (34–76)	62 (39–75)
Female	32%	26%
High-risk cytogenetics: del(17p), t(4;14), t(14;16)	28%	21%
R-ISS stage III	5%	6%
CR or sCR at screening	25% (n = 16)	37% (n = 31)
CR at best response	51%	64% (p = 0.056)
MRD negativity at any timepoint	18%	17%
Median follow-up, months	30.1	28.1

Table 2. Characteristics of the randomised ALLG MM23 population. All 149 randomised patients, not the 38 who contributed plasma. Equivalent characteristics for the sub-cohort were unavailable. Source: Rees et al.

Plasma proteomics. All 76 samples were run on a single Olink Reveal plate alongside 5 plate controls and 12 samples from an unrelated cohort. 1,033 assays cleared assay-level quality control (Figure 2). One assay, SDHAF4, was dropped due to a quality-control warning. The sample in well E7 had low read depth but was carried forward following leave-one-out and sensitivity testing (Table 4). Olink records signal in NPX, a relative $\log_2$ scale anchored to plate controls. One NPX unit is equivalent to a two-fold difference in assay signal. NPX values lack reference ranges and cannot be compared among different proteins. Plate control normalisation was used in the primary statistical model. In sensitivity analysis, median centring was subsequently used to assess whether results were normalisation-dependent.

Statistical analysis. The statistical model utilised a difference-of-differences interaction fitted in limma with patient blocking. Each patient's six-month-minus-baseline change was calculated to remove time-invariant patient characteristics. The mean lenalidomide control-arm change was subtracted from the mean Selinexor-arm change to isolate the proteomic effect of Selinexor. Statistical significance was determined using the Benjamini–Hochberg false-discovery rate at 5% across all 1,033 proteins.

$$\Delta NPX[i] = NPX[i,6m] - NPX[i,baseline]$$

NPX is Normalised Protein Expression; i denotes the individual patient; 6m is six months post-ASCT; and baseline is the post-transplant starting point.

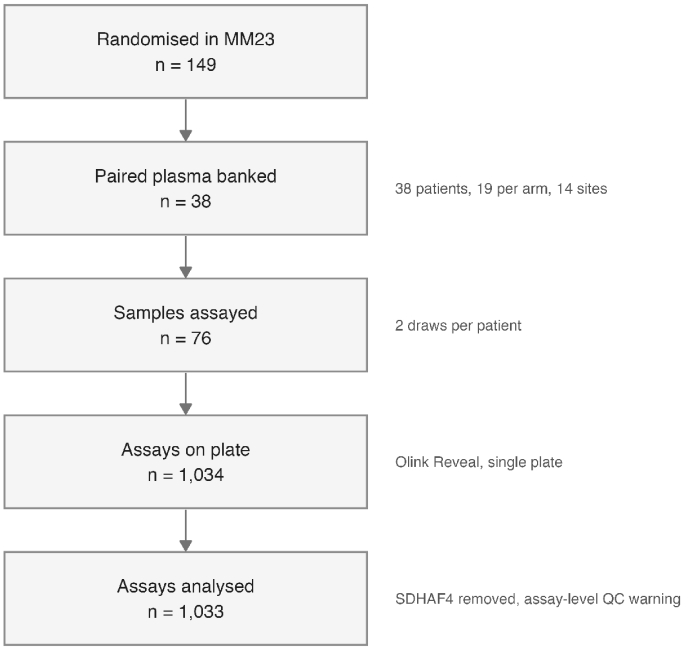

Figure 2. Cohort and assay schematic. Derivation of the analysed dataset from the randomised trial population. SDHAF4 was removed for an assay-level quality-control warning. E7 is retained.

3. Results

3.1 One assay of 1,033 survived correction

167 assays reached nominal $p < 0.05$, compared with 52 expected by chance alone. Benjamini–Hochberg correction was used to separate biological signal from noise. Under Benjamini–Hochberg correction, thrombopoietin was the sole assay to clear the 5% global false-discovery rate threshold ($q < 0.05$), with an interaction estimate of +1.197 $\log_2$ (95% CI 0.778–1.615), $p = 2.26 \times 10^{-7}$, $q = 2.33 \times 10^{-4}$ (Figure 3, Table 3). Ranks 2 to 10 fail correction, and effect sizes do not follow rank order (Table 3).

Rank	Assay	Effect ($\log_2$)	q	ρ with ΔTHPO
1	THPO	+1.197	2.33×10^{-4}	—
2	PDCD1LG2	+0.418	0.065	+0.46
3	UNG	+0.872	0.065	−0.26
4	FLT3LG	+0.757	0.065	+0.55
5	RASGRP2	−1.088	0.065	−0.37
6	SIGLEC7	+0.336	0.065	+0.57
7	ATRAID	+0.583	0.065	+0.12
8	PRTG	+0.396	0.065	+0.64
9	FKBP10	+0.617	0.065	+0.36
10	ITPR1	−0.761	0.065	−0.50

Table 3. The ten smallest interaction p-values. Rank-specific Benjamini–Hochberg threshold is $k \times 0.05/1{,}033$; only rank 1 falls below it. ρ is the post hoc exploratory Spearman correlation of each assay's within-patient change with ΔTHPO in the treated arm (n = 19). q-values are rounded to three decimals.

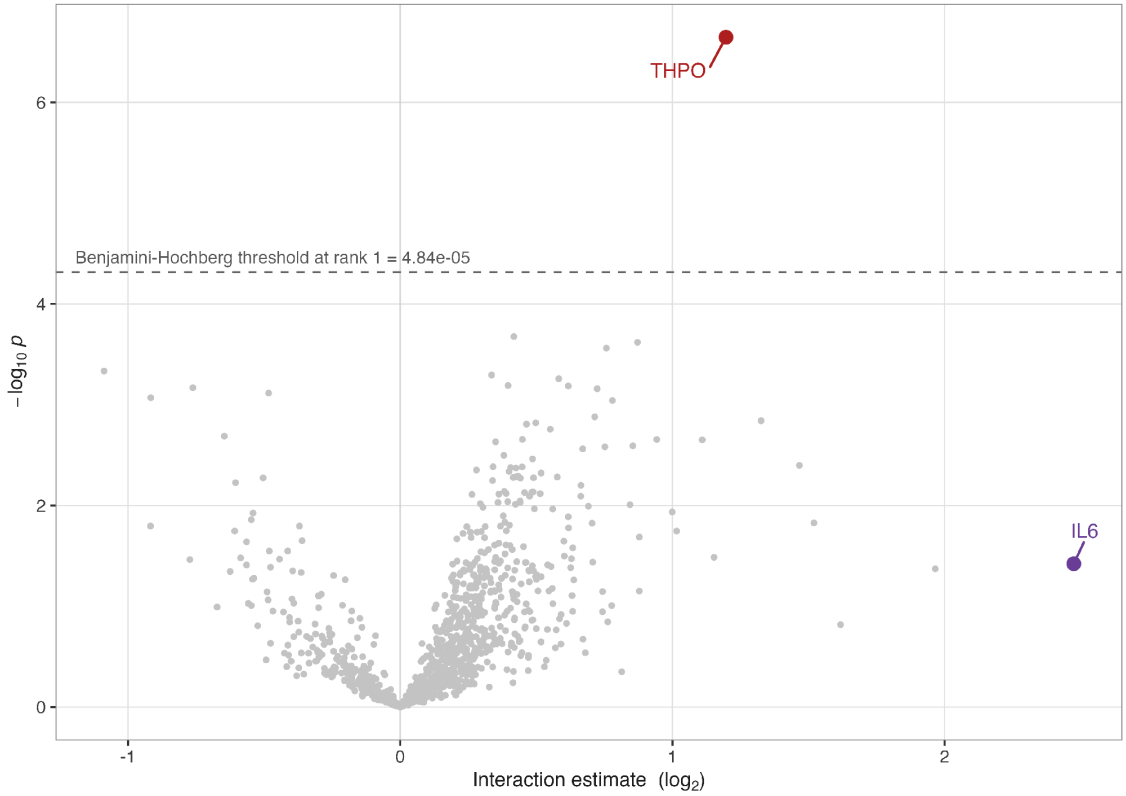

Figure 3. Arm × time interaction estimates for all 1,033 assays on the panel. The horizontal axis represents the estimated interaction coefficient in log_2 NPX units. The vertical axis is −log10 of the unadjusted p-value. Each point represents an individual assay. The dashed line marks the rank-1 Benjamini–Hochberg p-value threshold (4.84×10^{-5}) and applies only to rank 1; it is not a uniform significance boundary for the other points, because the Benjamini–Hochberg threshold rises with rank. Two assays are labelled, THPO and IL-6. IL-6 is labelled as it has the largest effect estimate in the panel (+2.47 log_2), with the largest standard error (1.17), compared with THPO's 0.21.

3.2 Direction of change was consistent across treated patients

The most striking change was that patients on selinexor showed a greater mean increase in THPO than the control arm. However, investigating means alone inevitably compresses the story. All 19 selinexor patients had a non-negative intra-patient change in THPO (median +1.013; interquartile range +0.671 to +1.548; minimum +0.010; maximum +2.596). In the control arm, change was more variable, with 9 of 19 controls rising (median: −0.048; range: −0.722 to +0.813). Considering this, the control arm's mean of −0.023 NPX is not a uniform result, and instead reflects cancellation rather than absence of movement (Figure 4A, 4B).

The ability of intra-patient THPO changes to discriminate between the randomised arms was evaluated using AUC, yielding 0.945 (Figure 4C). THPO achieved the highest AUC across all 1,033 assays. Within this

n=38 subcohort, an AUC of 0.945 indicates that, when selecting one treated patient and one control patient at random, the treated patient's THPO will have increased more than the control's in 94.5% of cases. To assess whether the obtained results were robust to specific analytical choices, sensitivity analyses were performed, yielding treatment effect estimates for THPO ranging from +1.037 to +1.332 log_2 fold change (Table 4).

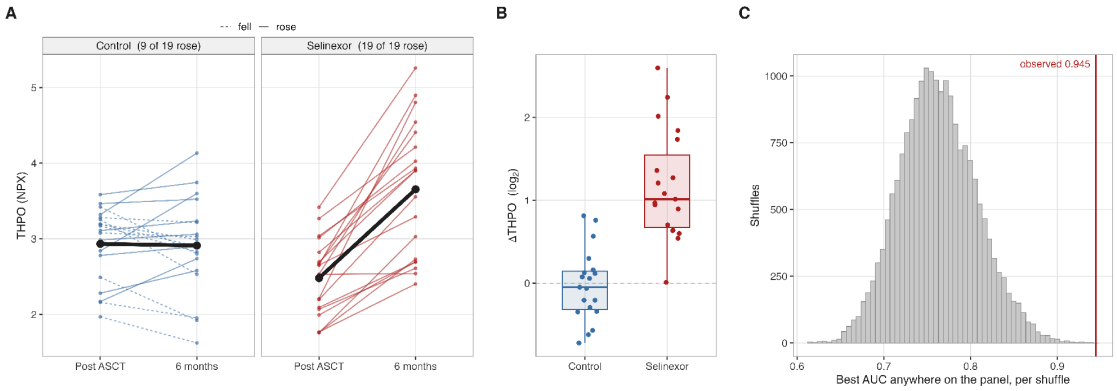

Figure 4. Per-patient change and permutation testing. (A) THPO NPX by timepoint and arm, n = 19 per arm; each line is one patient. Line style encodes the direction of change (solid: increased; dashed: decreased). In the selinexor arm, no line is dashed, since all 19 changes were non-negative; one change was approximately zero. Heavy lines denote arm means. (B) Intra-patient change by arm. Boxes show median and interquartile range. Treated arm median +1.013 (IQR +0.671 to +1.548, range +0.010 to +2.596); control median −0.048 (range −0.722 to +0.813).
(C) Arm labels were reassigned at random 20,000 times, producing versions of the data in which allocation carries no treatment information. Null distribution of the maximum arm-separation statistic across all 1,033 assays under these patient-level permutations, with the observed THPO value marked. No permutation exceeded the observed value of THPO.

Analysis	Source of bias addressed	Estimate (log_2)	Statistic
Primary interaction model	—	+1.197	q = 2.33×10^{-4} (BH, 1,033 assays)
Leave-one-out, 38 refits	Single influential patient	1.118 to 1.261	rank 1 of 1,033 in all 38 refits
Per-patient median removed	Per-sample loading or dilution	+1.048	p = 7.6×10^{-6} (unadjusted)
Median-centred normalisation	Plate-control anchor	+1.037	q = 6.3×10^{-3} (BH, 1,033 assays)
ANCOVA, baseline-adjusted (Δ ~ arm + baseline THPO)	Baseline imbalance between arms	+1.239	p = 4.7×10^{-7} (unadjusted)
Site-adjusted (Δ ~ arm + site, 14 fixed levels)	Recruitment centre	+1.186	p = 2.5×10^{-5} (unadjusted)
Plate-position adjusted (Δ ~ arm + row + column of both draws)	Spatial position on the single plate	+1.242 to +1.332	p = 1.7×10^{-7} to 1.1×10^{-6} (unadjusted)

Table 4. Sensitivity analyses applied to THPO. Six reanalyses of the same 38 patients, spanning estimates from +1.037 to +1.332 log_2. These assess sensitivity to specified analytical choices and do not provide independent validation.

3.3 THPO change and the single recorded grade ≥3 event

Given the overall rise in THPO within the selinexor arm, it is interesting to correlate the observed change in THPO with observed graded clinical events. Within this sub-cohort (n = 38), only one treated patient met recorded grade ≥3 thrombocytopenia criteria during the observation period. That patient's THPO change was +0.895 $\log_2$, below the arm median of +1.013, with twelve event-free patients changing more (Figure 5).

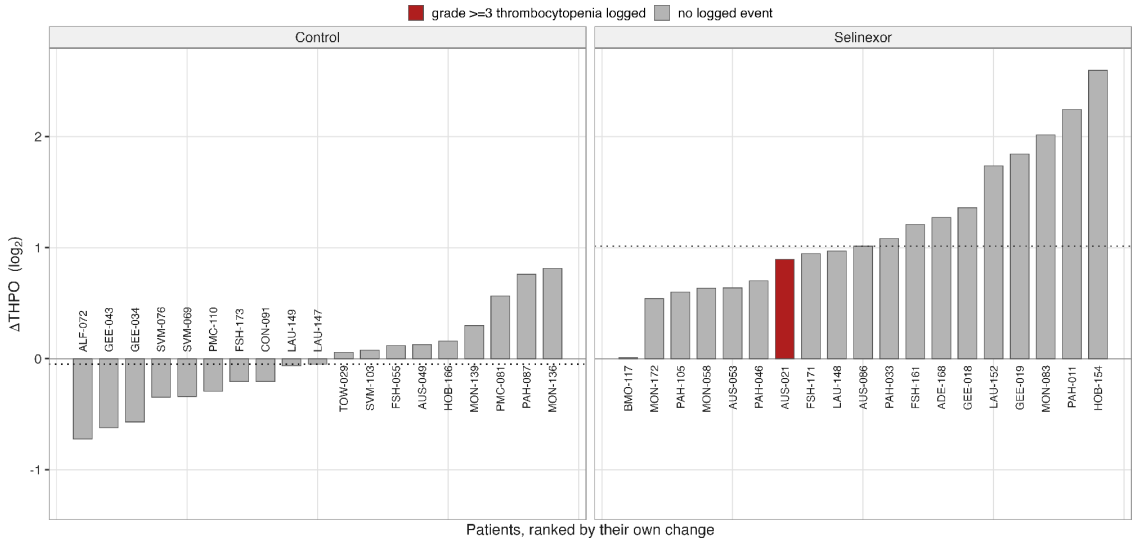

Figure 5. Within-patient ΔTHPO ranked by arm. Each bar represents one patient in the subcohort (n = 19 per arm), ordered by change in THPO. Patient AUS-021 is the sole patient with recorded grade ≥3 thrombocytopenia (biobank record) and is labelled in red. Dotted lines are arm medians. This figure is purely exploratory and descriptive. It shows that the sole known clinical event of grade ≥3 thrombocytopenia did not coincide with the largest observed increase in THPO.

4. Discussion

4.1 A single hit, and the shape of the argument that follows

All interpretation is post hoc. Proteomic screening unearthed THPO as a single statistically robust needle in a haystack (+1.197 $\log_2$ NPX). It was not nominated in advance. The story that follows is a mechanistic integration that seeks to hypothesise the biology underlying the observed result.

Physiologically, THPO is the key regulator of thrombopoiesis. THPO also regulates haematopoietic stem-cell maintenance and early megakaryocytic progenitor expansion and differentiation (Dasouki et al.; Ng et al.). The pathway of megakaryopoiesis culminating in platelet production is briefly outlined in Figure 6. ALLG MM23, the trial from which these samples were drawn, reports thrombocytopenia as a major dose-limiting toxicity of Selinexor, which limits its clinical utility (Rees et al.; Table 1). The following discussion explores THPO's role in selinexor-associated thrombocytopenia, drawing on existing literature to postulate that circulating THPO is regulated by a tap-and-drain paradigm which maintains a dynamic equilibrium between hepatic synthesis and c-Mpl receptor-mediated clearance.

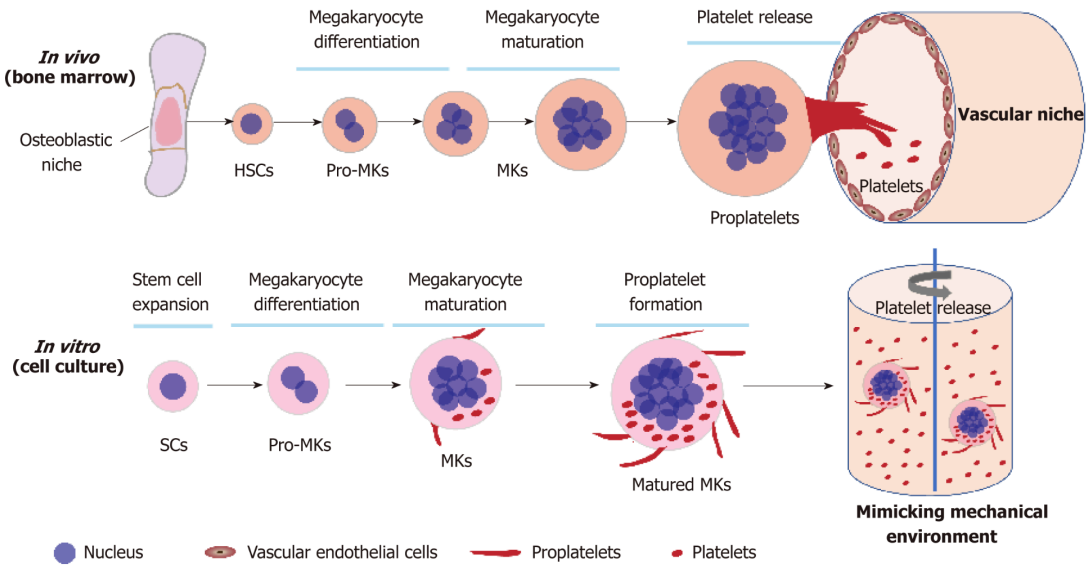

Figure 6. Megakaryopoiesis starts from haematopoietic stem cells and culminates in platelet biogenesis. Schematic of megakaryocyte differentiation, maturation and proplatelet formation in the bone marrow niche (upper) and the equivalent stages reproduced in vitro (lower). Source: Lei et al.

4.2 A tap and a drain

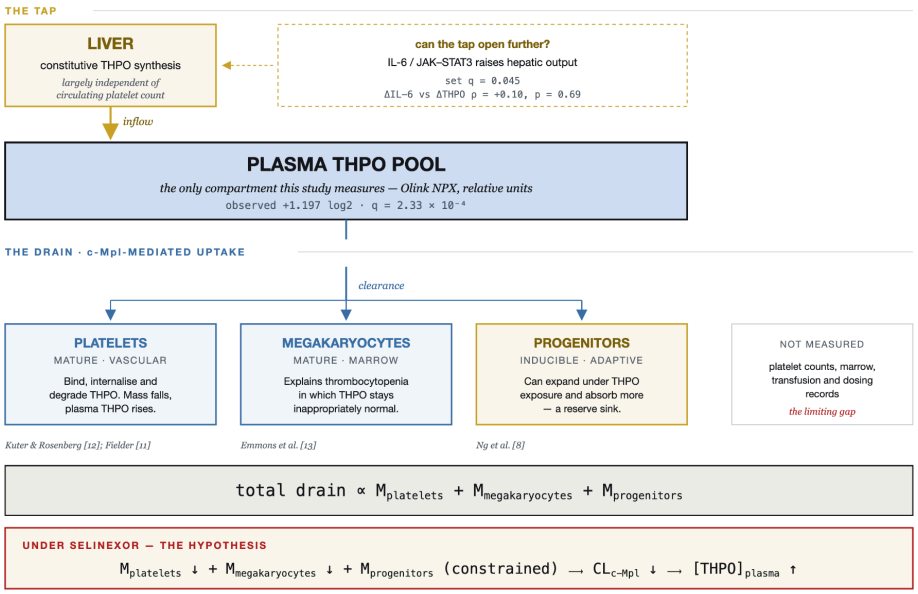

Figure 7. The tap-and-drain paradigm of plasma thrombopoietin. Constitutive hepatic secretion supplies the circulating THPO pool (the tap); c-Mpl-mediated binding, internalisation and degradation by platelets, megakaryocytes and progenitors removes THPO from it (the drain). A measured rise in plasma THPO is therefore consistent with either an open tap or a closed drain. Compartment evidence is drawn from Kuter and Rosenberg, Fielder et al., Emmons et al. and Ng et al.

The homeostatic regulation of THPO can be simplified using a tap-and-drain paradigm. The liver is the principal tap, constitutively secreting THPO into the circulation (Dasouki et al.; Grozovsky et al.; Sun et al.). To balance the tap, there must be a drain that removes THPO from circulation. That drain takes the form of c-Mpl, the cell-surface receptor for THPO, found on circulating platelets, marrow megakaryocytes, and early haematopoietic stem and progenitor cells (Fielder et al.; Ng et al.). Following THPO binding, c-Mpl-expressing cells internalise and degrade THPO, clearing it from the circulation (Fielder et al.; Kuter and Rosenberg). Within this paradigm, plasma THPO reflects the equilibrium between hepatic production and c-Mpl-mediated uptake and clearance (Figure 7).

$$Relative\ circulating\ THPO \propto \frac{Hepatic\ production\ ("tap")}{Effective\ c\text{–}Mpl\text{–}mediated\ uptake\ ("drain")}$$

c-Mpl is expressed on the THPO drain and can be defined as the aggregate functional c-Mpl-expressing mass of these compartments:

$$Total\ effective\ c\text{-}Mpl\text{-}mediated\ THPO\ drain \propto M_{platelets} + M_{megakaryocytes} + M_{progenitors}$$

M denotes functional c-Mpl-expressing mass, incorporating cell abundance, cell-surface c-Mpl availability, and the capacity for receptor-mediated internalisation and degradation. This is a conceptual rather than quantitative equation that acknowledges that the relative contribution of each compartment may vary with receptor density, THPO accessibility, and internalisation kinetics, none of which have been formally characterised.

The platelet and megakaryocyte compartments together form the main mature component of THPO uptake. By contrast, the progenitor compartment is potentially adaptive.

$$Mature\ THPO\text{-}uptake\ compartment = M_{platelets} + M_{megakaryocytes}$$

Increased THPO exposure may expand c-Mpl-expressing progenitors and increase their contribution to THPO uptake (Ng et al.).

4.3 Deconstructing the drain: evidence for three clearance compartments

$M_{platelets}$: Kuter and Rosenberg established an inverse relationship between platelet mass and circulating THPO using busulfan-treated rabbit models of thrombocytopenia (Kuter and Rosenberg). They observed that the decline in platelet mass was associated with a proportional increase in THPO, with THPO levels peaking at platelet nadir (Kuter and Rosenberg). Conversely, platelet transfusion resulted in a rapid decline in circulating THPO (Kuter and Rosenberg). *In vitro* incubation of rabbit platelets with thrombocytopenic plasma removed THPO, affirming that platelet-mediated THPO clearance can occur independently of whole-body regulation (Kuter and Rosenberg). In humans, Fielder et al. identified c-Mpl as the receptor involved in clearance, showing high-affinity binding of THPO to cell-surface c-Mpl receptors followed by internalisation and degradation of the ligand–receptor complex (Fielder et al.).

These studies characterise platelets as a key sink for THPO, but fail to explain cases of clinical thrombocytopenia in which THPO levels remain normal, prompting investigations of the upstream marrow compartment, since megakaryocytes also express c-Mpl.

$M_{megakaryocytes}$: Emmons et al. refined the platelet-centred model of THPO clearance by investigating clinical aetiologies of thrombocytopenia (Emmons et al.). They observed that circulating THPO concentrations are in part dependent on megakaryocyte mass (Emmons et al.). In thrombocytopenia due to megakaryocytic hypoplasia, serum THPO was markedly elevated, whereas in thrombocytopenia resulting from increased peripheral platelet destruction where marrow megakaryocyte mass was maintained, THPO remained low or undetectable (Emmons et al.). Biologically, platelets are downstream products of megakaryocytes (Figure 6). Hence, the THPO elevation seen in hypoplasia is not an isolated collapse of the megakaryocyte compartment but should instead be interpreted as a dual-compartment contraction. Hypoplasia depletes the upstream megakaryocyte sink, thereby reducing downstream platelet production and slashing overall c-Mpl mass in both mature compartments. Ultimately, Emmons' findings demonstrate that THPO regulation is not solely platelet-dependent, but rather reflects the aggregate c-Mpl-expressing mass of both compartments.

$M_{progenitors}$: Studies by Ng et al. identify a third compartment using $Mpl^{PF4cre/PF4cre}$ mice in which PF4 promoter-driven Cre recombinase deleted Mpl in late megakaryocyte progenitors, megakaryocytes, and platelets, while sparing Mpl expression in earlier stem and progenitor populations (Ng et al.).

Compared with $Mpl^{fl/fl}$ controls, $Mpl^{PF4cre/PF4cre}$ mice exhibited pronounced megakaryocytosis and thrombocytosis (Ng et al.). This means that although, in absolute terms, the mature megakaryocyte and platelet compartments in the $Mpl^{PF4cre/PF4cre}$ mice expanded quantitatively, the very nature of the deletion meant that this expanded cell population lacked c-Mpl, resulting in reduced c-Mpl receptor mass across these compartments. Paradoxically, despite this c-MPL deficiency, circulating THPO levels remained comparable to controls, and hepatic THPO transcription was unaltered (Ng et al.). Instead, it was observed that the genetically c-Mpl-expressing multipotent and megakaryocyte-committed progenitors expanded under THPO stimulation. Ng et al. proposed that decreased THPO uptake by mature c-Mpl-deficient cells increases the availability of cytokines to upstream progenitors (Ng et al.). The expansion of these early progenitors functions as an adaptive reserve that subsequently increases the overall capacity for receptor-mediated internalisation and consumption (Ng et al.). This cellular expansion ultimately buffers circulating THPO levels despite the persistent loss of c-Mpl expression in mature cells (Ng et al.).

The above findings characterise the different potential sinks that regulate THPO clearance. The third compartment is a hypothesised sink inferred from a mouse genetic model rather than one measured in humans, and the contribution of specific individual progenitor populations to systemic THPO clearance was not characterised (Ng et al.).

4.4 Selinexor as a possible pharmacological disruption of adaptive THPO regulation

The inducible progenitor compartment described by Ng et al. provides a framework for interpreting Selinexor-associated thrombocytopenia. Because Selinexor impairs early megakaryocytic progenitor differentiation, it could restrict the expansion and replenishment of the very progenitor compartment that provided adaptive buffering in $Mpl^{PF4cre/PF4cre}$ mice (Machlus et al.; Ng et al.).

Studies in murine models by Machlus and colleagues demonstrated that Selinexor inhibits XPO1-dependent nuclear export and increases nuclear localisation of phosphorylated STAT3 (pSTAT3) in early megakaryocytic progenitors *in vitro* (Machlus et al.). Nuclear retention of pSTAT3 was associated with upregulation of the stem cell-like factors Klf4 and subsequently Oct4, which blocked early megakaryocytic differentiation and maturation (Machlus et al.). Mature megakaryocyte viability and

proplatelet formation were not significantly affected in their models (Machlus et al.). Machlus postulated that Selinexor-associated thrombocytopenia arises predominantly from a stage-specific failure of early megakaryopoiesis, rather than from direct destructive or lytic clearance of mature megakaryocytes or circulating platelets (Machlus et al.).

Interpreted within the context of thrombopoiesis, the terminal output of megakaryopoiesis, sustained inhibition of early megakaryocytic differentiation would block upstream pathways, reduce the generation of new megakaryocytes, and subsequently reduce circulating platelets, progressively decreasing the mature components of c-Mpl-mediated THPO uptake (Emmons et al.; Kuter and Rosenberg). If Selinexor simultaneously constrains c-Mpl-expressing progenitors, it would also disable the adaptive uptake reserve observed in the Ng model, producing a coordinated, multi-compartment depletion of the total body receptor sink (Machlus et al.; Ng et al.):

$$M_{platelets} \downarrow + M_{megakaryocytes} \downarrow + M_{progenitors}\ (constrained) \longrightarrow CL_{c\text{-}Mpl} \downarrow \longrightarrow [THPO]_{plasma} \uparrow$$

The observed 1.197 $\log_2$ relative increase in THPO within the Selinexor maintenance arm aligns with a treatment-induced reduction in net c-Mpl-mediated THPO uptake. However, this interpretation must be taken with a grain of salt regarding its direct applicability to the underlying Olink results. While Machlus et al. established that Selinexor induces differentiation arrest in cultured megakaryocyte progenitors in vitro, it has not formally established whether a once-weekly maintenance dose (at a mean relative intensity of 55% in the MM23 trial) causes sufficient progenitor loss or functional impairment in human bone marrow to completely collapse the inducible sink (Rees et al.).

Returning to clinical outcome data. Only one patient within the sub-cohort had a recorded grade ≥3 thrombocytopenia event, which complicates the reading of the tap-and-drain paradigm. If plasma THPO were a straightforward inverse function of depleted platelet mass, the patient with the most severe recorded thrombocytopenia (AUS-021, +0.895 $\log_2$) would be expected to show one of the largest THPO increases, but it does not.

4.5 Returning to the Tap. Considering an alternative mechanism: increased hepatic THPO production

Homeostasis is a two-way street. Returning to the tap, increased hepatic THPO synthesis represents an alternative explanation for the observed THPO signal in the Selinexor arm.

Gene-set enrichment analysis identified an increase in inflammatory-response signalling (q = 0.007) and IL-6/JAK–STAT3 signalling (q = 0.045) within the Selinexor arm (Figure 8). This is mechanistically relevant because IL-6 is an established stimulus of hepatic THPO production, providing a pathway through which inflammation may influence THPO levels independent of c-Mpl-mediated clearance (Kaser et al.). JAK2 further regulates hepatic THPO production via STAT3 signalling downstream of the Ashwell–Morell receptor and by hepatocyte Notch1 signalling, so the liver tap cannot be blindly read as a fixed constant (Grozovsky et al.; Sun et al.).

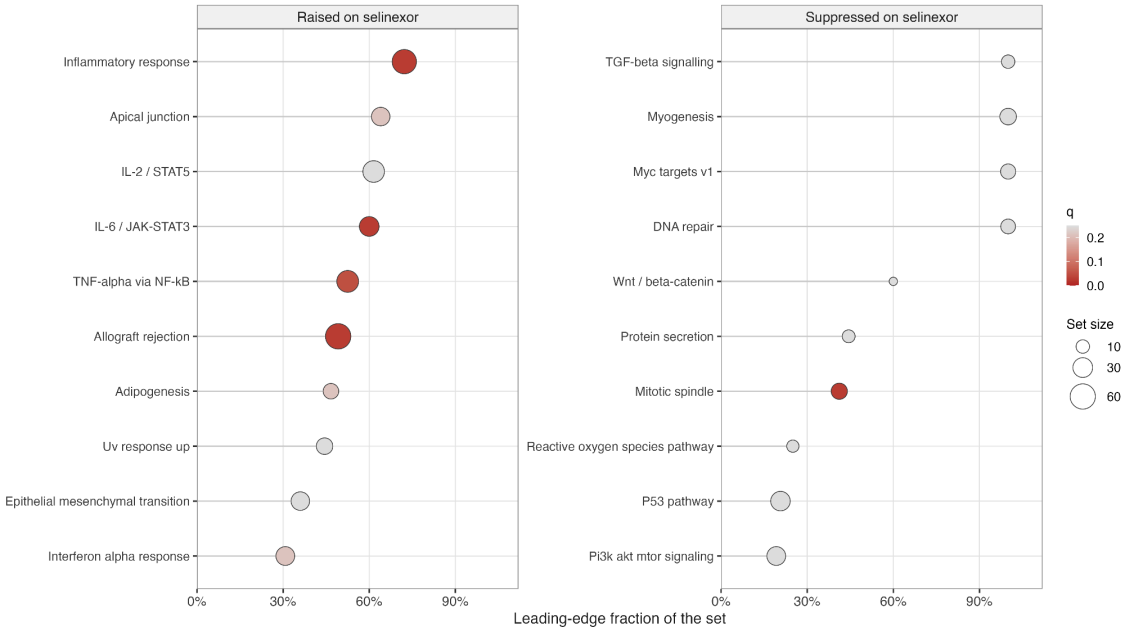

Figure 8. Hallmark gene sets ranked by leading-edge fraction. The horizontal axis is the proportion of set members falling in the leading edge of the ranked interaction statistic; dot area is the number of set members measured on the panel; fill is the Benjamini–Hochberg q-value from gene-permutation GSEA. Sets with fewer than five panel members were not tested.

To investigate this further, intra-patient changes in THPO and IL-6 were plotted. Intra-patient changes in IL-6 and THPO did not correlate in either the selinexor arm ($\rho = +0.10$, $p = 0.69$) or the control arm ($\rho = -0.07$, $p = 0.77$) (Figure 9). The patient with the largest THPO increase (HOB-154, +2.6 $\log_2$ NPX) ranked 15th of 19 for IL-6 change and showed a net decrease in IL-6 over the six-month interval. The participant with the largest IL-6 increase (PAH-011, +9.9 $\log_2$ NPX) ranked second for THPO change. While these observations do not support a strong patient-level correlation between circulating IL-6 and THPO in this dataset, they also cannot rule out IL-6-driven hepatic synthesis due to study limitations and small sample size. A two-timepoint plasma snapshot taken six months apart cannot capture transient systemic inflammatory spikes in the interval, nor localised microenvironmental IL-6 activity in the bone marrow or liver.

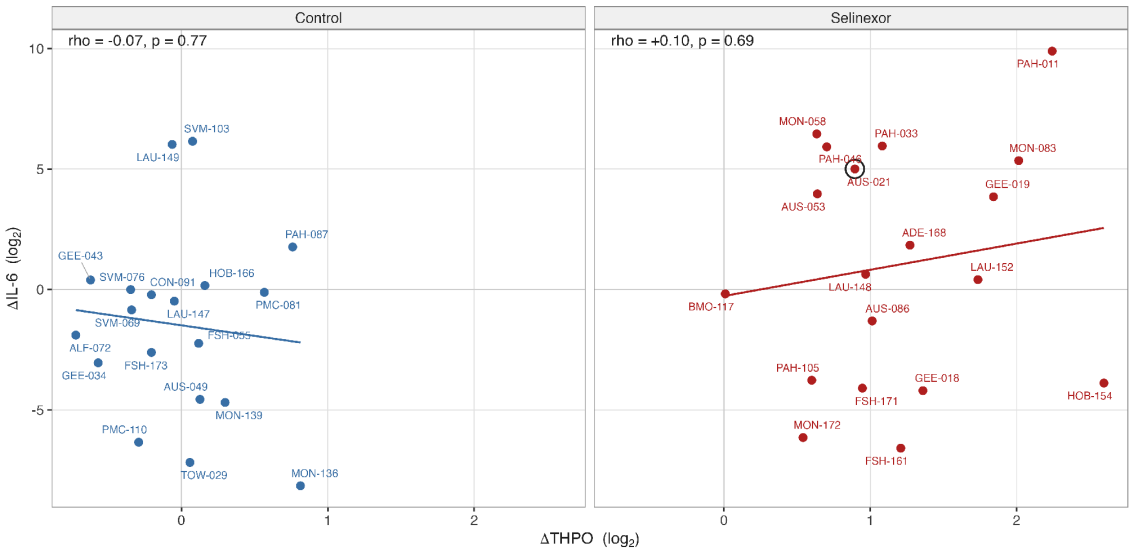

Figure 9. Within-patient ΔIL-6 against ΔTHPO, by arm. n = 19 per arm; lines, ordinary least-squares fits within arm; ρ, Spearman with exact p. Circled, the patient meeting grade ≥3 thrombocytopenia criteria. Treated arm ρ = +0.10 (p = 0.69); control ρ = −0.07 (p = 0.77).

Considering the existing literature characterised above in tandem with the MM23 Olink results, it is postulated that the increased THPO signal observed during Selinexor maintenance in this dataset is likely multifactorial, reflecting changes in c-Mpl-mediated clearance, increased hepatic THPO production, or a combination of both mechanisms.

4.6 Limitations and future directions

This study represents a discovery-stage, post-hoc analysis. The results are hypothesis-generating and not conclusive. The two-timepoint sampling design prevents assessment of whether changes in THPO preceded, accompanied, or followed platelet decline, treatment modification, or clinically significant thrombocytopenia. The absence of serial platelet counts, adverse-event timing, and demographic covariates further limits mechanistic inference.

Individual patient data were not available at the time of analysis. The trial protocol acknowledges the use of concomitant medications, specifying that thrombopoietin receptor agonists and transfusions may be used to manage chemotherapy-induced thrombocytopenia. Due to the absence of definitive per-patient data, neither agonist exposure nor platelet transfusion can be excluded, making it infeasible to determine whether these variables contributed to the observed THPO signal.

The Olink findings are limited in generalizability due to heterogeneity in Selinexor exposure, with a mean relative dose intensity of 55% and an average of 9 Selinexor-containing cycles per patient (range 1-34) (Rees et al.). Additionally, the inability to account for other potential confounding factors at the individual patient level, such as thrombocytopenia from lenalidomide, marrow involvement from myeloma, infections, corticosteroid exposure, and hepatic or renal dysfunction, further restricts interpretation due to the lack of per-patient data.

Relative Olink NPX measurements do not quantify absolute THPO concentrations and cannot distinguish between increased hepatic production and decreased c-Mpl-mediated THPO uptake or clearance. The mechanism of impaired progenitor cell adaptation is primarily supported by a conditional mouse model (Ng et al.) and an in vitro cell culture model (Machlus et al.), rather than by data from patients treated with selinexor. Furthermore, it has been characterised that platelet release is not exclusively THPO-dependent, as IL-1-driven megakaryocyte rupture can generate platelets independently of THPO signalling (Nieswandt and Stritt).

Addressing these limitations requires access to individual patient records. The ALLG MM23 protocol indicates that the regulatory biobank has obtained patient-level bone marrow biopsies, serial complete blood counts, and medication histories. Recommended next steps include: (1) performing quantitative ELISA validation of absolute THPO concentration (pg/mL) to confirm that changes in NPX reflect actual changes in circulating protein levels; (2) correlating serial platelet counts with THPO trajectory to determine whether changes in THPO precede or follow platelet decline; and (3) conducting flow cytometric analysis of surface c-Mpl expression on CD34+ progenitor cells in bone marrow cultures exposed to selinexor in vitro to further investigate the progenitor component of the model.

5. Conclusion

This exploratory analysis of paired plasma from 38 participants in a randomised maintenance trial returned THPO as the sole statistically significant arm-by-time difference among 1,033 assayed proteins ($+1.197$ $\log_2$ NPX; $q = 2.33 \times 10^{-4}$), with estimates ranging from +1.037 to +1.332 across six reanalyses of the same data. The direction of change was consistent across all 19 selected patients. Whether this reflects reduced c-Mpl-mediated clearance, increased hepatic production, or both cannot be determined from these data, and the mechanistic account offered above is a hypothesis to be tested rather than a finding.

Works Cited

Argueta, Christian, et al. “Selinexor Synergizes with Dexamethasone to Repress mTORC1 Signaling and Induce Multiple Myeloma Cell Death.” *Oncotarget*, vol. 9, no. 39, May 2018, pp. 25529–44. *DOI.org (Crossref)*, https://doi.org/10.18632/oncotarget.25368.

Dasouki, Majed, et al. “THPO-MPL Pathway and Bone Marrow Failure.” *Hematology/Oncology and Stem Cell Therapy*, vol. 8, no. 1, Jan. 2015, pp. 6–9. *DOI.org (Crossref)*, https://doi.org/10.1016/j.hemonc.2014.11.005.

Emmons, Rv, et al. “Human Thrombopoietin Levels Are High When Thrombocytopenia Is Due to Megakaryocyte Deficiency and Low When Due to Increased Platelet Destruction.” *Blood*, vol. 87, no. 10, May 1996, pp. 4068–71. *DOI.org (Crossref)*, https://doi.org/10.1182/blood.V87.10.4068.bloodjournal87104068.

Fielder, Paul J., et al. “Human Platelets as a Model for the Binding and Degradation of Thrombopoietin.” *Blood*, vol. 89, no. 8, Apr. 1997, pp. 2782–88. *DOI.org (Crossref)*, https://doi.org/10.1182/blood.V89.8.2782.

Grozovsky, Renata, et al. “The Ashwell-Morell Receptor Regulates Hepatic Thrombopoietin Production via JAK2-STAT3 Signaling.” *Nature Medicine*, vol. 21, no. 1, Jan. 2015, pp. 47–54. *DOI.org (Crossref)*, https://doi.org/10.1038/nm.3770.

Kaser, Arthur, et al. “Interleukin-6 Stimulates Thrombopoiesis through Thrombopoietin: Role in Inflammatory Thrombocytosis.” *Blood*, vol. 98, no. 9, Nov. 2001, pp. 2720–25. *DOI.org (Crossref)*, https://doi.org/10.1182/blood.V98.9.2720.

Kuter, Dj, and Rd Rosenberg. “The Reciprocal Relationship of Thrombopoietin (c-Mpl Ligand) to Changes in the Platelet Mass during Busulfan-Induced Thrombocytopenia in the Rabbit.” *Blood*, vol. 85, no. 10, May 1995, pp. 2720–30. *DOI.org (Crossref)*, https://doi.org/10.1182/blood.V85.10.2720.bloodjournal85102720.

Lei, Xiao-Hua, et al. “Induction of Differentiation of Human Stem Cells *Ex Vivo* : Toward Large-Scale Platelet Production.” *World Journal of Stem Cells*, vol. 11, no. 9, Sept. 2019, pp. 666–76. *DOI.org (Crossref)*, https://doi.org/10.4252/wjsc.v11.i9.666.

Machlus, Kellie R., et al. “Selinexor-Induced Thrombocytopenia Results from Inhibition of Thrombopoietin Signaling in Early Megakaryopoiesis.” *Blood*, vol. 130, no. 9, Aug. 2017, pp. 1132–43. *DOI.org (Crossref)*, https://doi.org/10.1182/blood-2016-11-752840.

Ng, Ashley P., et al. “Mpl Expression on Megakaryocytes and Platelets Is Dispensable for Thrombopoiesis but Essential to Prevent Myeloproliferation.” *Proceedings of the National Academy of Sciences*, vol. 111, no. 16, Apr. 2014, pp. 5884–89. *DOI.org (Crossref)*, https://doi.org/10.1073/pnas.1404354111.

Nieswandt, Bernhard, and Simon Stritt. “Megakaryocyte rupture for acute platelet needs.” The Journal of cell biology vol. 209,3 (2015): 327-8. doi:10.1083/jcb.201504026

Rees, Matthew, et al. “Primary Analysis of the Phase 3 Randomized Trial of Selinexor and Lenalidomide versus Lenalidomide Alone as Maintenance Therapy Post Autologous Stem Cell Transplant for Patients with Newly Diagnosed Multiple Myeloma (ALLG MM23; SEALAND).” *Blood*, vol. 146, no. Supplement 1, Nov. 2025, pp. 4039–4039. *DOI.org (Crossref)*, https://doi.org/10.1182/blood-2025-4039.

Sun, Yueyue, et al. “Notch1 Regulates Hepatic Thrombopoietin Production.” *Blood*, vol. 143, no. 26, June 2024, pp. 2778–90. *DOI.org (Crossref)*, https://doi.org/10.1182/blood.2023023559.

Tai, Y. T., et al. “CRM1 Inhibition Induces Tumor Cell Cytotoxicity and Impairs Osteoclastogenesis in Multiple Myeloma: Molecular Mechanisms and Therapeutic Implications.” *Leukemia*, vol. 28, no. 1, Jan. 2014, pp. 155–65. *DOI.org (Crossref)*, https://doi.org/10.1038/leu.2013.115.

Walker, Janek S., et al. “Recurrent XPO1 Mutations Alter Pathogenesis of Chronic Lymphocytic Leukemia.” *Journal of Hematology & Oncology*, vol. 14, no. 1, Dec. 2021, p. 17. *DOI.org (Crossref)*, https://doi.org/10.1186/s13045-021-01032-2.